European Journal of Gynaecological Oncology

IMR Press

Original Research

Bioinformatic analysis identifies potential key genes in the pathogenesis of uterine leiomyoma

Yi-Chao Jin[1,†], Tong-Hui Ji[1,†], Xiong Yuan[1], Ying Sun[1], Yu-Jie Sun[2], Jie Wu[1,*]

[1] *Department of Gynecology, The First Affiliated Hospital of Nanjing Medical University, Nanjing, 210029 Jiangsu, P. R. China*

[2] *Key laboratory of Human Functional Genomics of Jiangsu Province, Nanjing Medical University, Nanjing, 211126 Jiangsu, P. R. China*

*Correspondence: wujiemd@126.com (Jie Wu)

† These authors contributed equally.

DOI:10.31083/j.ejgo.2021.01.2151

Submitted: May 25, 2020 Revised: August 12, 2020 Accepted: August 28, 2020 Published: February 15, 2021

Objective: The present study aimed to screen hub genes for pathology of uterine leiomyoma. *Methods*: The microarray data of GSE31699, containing 16 uterine leiomyoma tissue samples and 16 matched normal myometrium samples, were downloaded from the Gene Expression Omnibus database (GEO). The "limma" R language package was used to identify differently-expressed genes (DEGs) between uterine leiomyoma and myometrium. Gene Ontology (GO) and pathway enrichment analyses were performed by using clusterprofiler, the DEGs were mostly enriched in post-synapse assembly, response to glucocorticoid, extracellular matrix receptor interaction and coagulation cascades. Subsequently, a protein-protein interaction (PPI) network of DEGs was constructed by Search Tool for the Retrieval of Interacting Genes Database (STRING) and visualized by utilizing Cytoscape software. We screened hub clusters of PPI network by the plug-in Molecular Complex Detection (MCODE) in Cytoscape, then clusterprofiler was also utilized to analyze functions and pathways enrichment of the genes in the hub clusters. Furthermore, we employed the "WGCNA" package in R to conduct co-expression network for all genes in GSE31699. Ultimately, we selected the overlapped genes in hub clusters of DEGs' PPI network and WGCNA. *Results*: Five genes (*COL5A2*, *ALDH1A1*, *GNG11*, *EFEMP1*, *ANXA1*) were finally validated in other GEO datasets (GSE64763, GSE764, GSE593) and Oncomine database. Gene set enrichment analysis (GSEA) was also performed for the hub genes. The expression of *COL5A2* was significantly higher in uterine leiomyoma compared with that in myometrium, while the expression of the other hub genes was significantly lower in uterine leiomyoma. *Conclusion*: The results indicated that *COL5A2*, *ALDH1A1*, *GNG11*, *EFEMP1* and *ANXA1* may be the key pathological genes in uterine leiomyoma.

Keywords

Bioinformatics analysis; Uterine leiomyoma; PPI; WGCNA

1. Introduction

Uterine leiomyomas, also called myomas or uterine fibroids, are the most common benign neoplasms of the uterus, which consist of smooth muscle and varying amounts of fibrous tissue. The estimated lifetime prevalence of uterine leiomyomas approaches as high as 70%-80%. Most patients with uterine fibroids have no obvious symptoms. 30% of cases may present with abnormal uterine bleeding (heavy menstrual bleeding, prolonged menstruation, anemia), pelvic mass and compression symptoms (dysuria, constipation, hydronephrosis), pelvic pain, infertility and pregnancy complications [1]. Although the rate of malignant transformation is low, uterine fibroids are still a tremendous public health burden and the most frequent indication for hysterectomy [2].

Traditionally, it is universally acknowledged that uterine fibroids are clonal smooth muscle cell neoplasms, and gonadal steroids play an important role in their occurrence and development. Some uterine fibroids also have specific molecular genetic background and chromosomal rearrangement [3]. The latest research shows that at least four types of cellular components exist in uterine fibroids: uterine smooth muscle cells, vascular smooth muscle cells, fibroblasts, and fibroid-associated fibroblasts. All of these cells are derived from fibroid progenitor cells which are transformed from myometrial stem cells [4]. In addition, the excessive accumulated extracellular matrix (ECM) including collagens is also an important constituent of uterine fibroids [5]. Compared with normal myometrium, the amount and topological structure of extracellular matrix in uterine fibroids have changed significantly. Besides, the cellular components can secrete growth factors, cytokines, chemokines, proteases, angiogenic and inflammatory response mediators locally in an autocrine or paracrine manner. These molecules may account for the development of uterine fibroids by promoting cell proliferation, angiogenesis, inflammation and ECM accumulation [6]. However, the precise molecular mechanisms and cellular changes of uterine fibroids have not been comprehensively elucidated and effective treatment is limited by the poor understanding of their pathogenesis.

Currently, bioinformatic analysis has been extensively used to explore pivotal genes related to different diseases including uterine leiomyomas. For example, Liu and coworkers revealed the potential role of *CASP1*, *ALDH1A* and *PROS1* in uterine leiomyoma diagnosis and treatment by using GEO database [7]. And the location of the uterine leiomyoma may have a different gene expression profile [8]. In this study,

weighted gene expression network analysis (WGCNA) was carried out given that only concerning about the genes' discrepant expression may neglect the potential association among genes. WGCNA is a systematic biological method for describing the correlation patterns among genes across microarray samples. It can be used for identifying modules of highly associated genes, candidate biomarkers or therapeutic targets according to associations of each modules and relationships between modules and external sample phenotypes [9]. In our study, we identified hub genes by both WGCNA analysis and DEG's PPI network construction. These hub genes and related pathways may contribute to the pathology of uterine leiomyomas or may be potential therapeutic targets in the future.

2. Materials and methods

2.1 Ethics statement

This study was a bioinformatical research, and all procedures followed were in accordance with the ethical standards of the responsible committee on human experimentation (institutional and national).

2.2 Microarray data and preprocessing

GEO (http://www.ncbi.nlm.nih.gov/geo/) is a public functional genomics database which provides array- and sequence-based data. Gene expression dataset GSE31699 was performed by Illumina HumanHT-12 V3.0 expression beadchip. We downloaded the dataset from GEO and converted the probes into the matching gene symbol in accordance with the annotation information in the platform. The GSE31699 dataset included 16 uterine leiomyoma tissue samples and 16 matched normal myometrium samples. According to the original study, the patients were all African American premenopausal women (mean age 44 years; range 30-50 years) without any hormonal treatment for at least 6 months prior to surgery, and the tumor sizes ranged from 5 to 17 cm in diameter. And there was no detailed information on the molecular genetic background of the uterine leiomyoma samples.

2.3 Study design & data processing

We designed the study on the basis of the flow diagram (Fig. 1). We evaluated the data quality by sample clustering based on the Pearson's correlation matrices between different samples. In addition, a heatmap was drawn according to the different expressions of probes (Fig. S1). According to the clustering results and heatmap, we deleted the samples GSM786796 and GSM786789 to eliminate the potential bias in the subsequent analysis.

2.4 Differentially expressed genes

We employed the "limma" R language package to screen the DEGs between uterine leiomyoma and normal myometrium [10]. The adjusted P-value < 0.05 and $|\log2\text{fold change (FC)}| > 1$ were considered statistically significant.

2.5 KEGG and GO enrichment analyses of DEGs

Gene Ontology (GO, http://geneontology.org/) provides an ontology of defined terms to represent gene functions (molecular function, cellular component and biological process). Besides, Kyoto Encyclopedia of Genes and Genomes (KEGG, http://www.genome.jp/kegg/) is a database resource for understanding high-level functions and utilities of the biological system. A package in R language called "clusterprofiler" was used to determine the biological significance of DEGs. The package is capable of providing GO and KEGG enrichment analyses and visualization for users to obtain more valuable biological information [11]. P value $<$ 0.05 was considered as a significant enrichment.

2.6 PPI network construction and clusters analyses

Search Tool for the Retrieval of Interacting Genes (http://string-db.org) (version 10.0) online database was utilized to predict PPI network of DEGs [12]. Then we converted the results into visualization by Cytoscape software [13]. Furthermore, we used the plug-in Molecular Complex Detection (MCODE) (version 1.4.2) in Cytoscape to select hub modules of PPI network. The degree cut-off = 2, node score cutoff = 0.2, k-core = 2, and Max depth = 100 were set as significant and the hub clusters were selected [14]. Subsequently, KEGG and GO analyses for genes in the hub clusters were performed by "clusterprofiler" package in R language.

2.7 Weighted co-expression network construction and module enrichment analyses

To investigate the differences between uterine leiomyoma and the matched adjacent normal myometrium, the co-expression network of GSE31699 was created and the module function was analyzed. Firstly, we tested the expression data profile and determined that the samples and genes are suitable. Secondly, the "WGCNA" package in the R language was employed to create the co-expression networks [15]. Thirdly, a power function amn = ((1+cmn)/2) ^ β (cmn = Pearson's correlation between gene m and gene n; amn = adjacency between gene m and gene n; β = soft-thresholding power) was used. And we established a weighted adjacency matrix. A soft-thresholding power β was utilized to highlight strong correlations between genes and attenuate weak associations. Fourthly, we switched the adjacency to topological overlap matrix (TOM) and measured network connectivity of each gene. Average linkage hierarchical clustering was created according to the TOM-based dissimilarity, and we set the minimum size of the genes dendrogram as 30. Thereby, genes with strong correlations were grouped into the corresponding gene module. Then, we figured out the dissimilarity of module eigengenes. To determine associated modules that may be involved in the pathogenesis of uterine leiomyoma, GO and KEGG enrichment analyses were employed on these gene modules.

2.8 Hub genes validation

Oncomine database (www.oncomine.org) is an online cancer microarray database for DNA or RNA sequence analysis, which was employed to analyze the transcription levels of selected hub genes in different cancers. The mRNA expressions of the genes in cancers including uterine leiomyoma

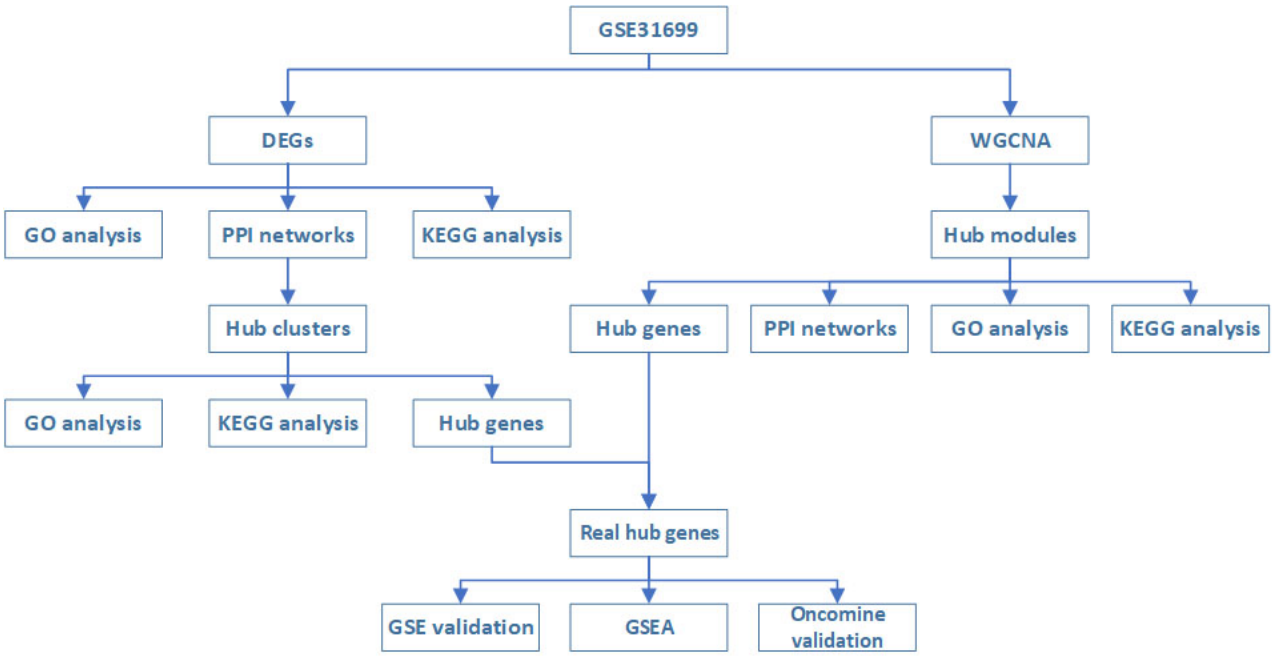

Fig. 1. Study design and the flow diagram of study.

were compared with those in normal controls by student's *t* test. Cut-off of *P* value and fold change were as following: *P* value: 0.01, fold change: 1.5, gene rank: 10%, data type: mRNA. In addition, other GEO datasets were also searched to validate the expression of the real hub genes.

2.9 Gene set enrichment analysis

To explore the potential functions of selected hub genes in uterine leiomyoma, samples of uterine leiomyoma dataset GSE31699 were divided into different groups in accordance with the expression levels of the 5 hub genes respectively. GSEA was utilized to explore whether priority determined biological processes datasets were enriched in these groups [16, 17]. The criteria were set as P value < 0.05 and FDR < 0.25.

3. Result

3.1 Identification of DEGs in uterine leiomyoma

We identified DEGs in GSE31699 by using limma package in R language after deleting the samples GSM786796 and GSM786789 as described previously. The DEGs were displayed in a volcano plot based on |log2FC| (Fig. S2). Then, we draw a heatmap of these DEGs which included 125 up-regulated genes and 148 down-regulated genes in leiomyoma tissues by comparison with normal myometrium tissues (Fig. 2).

3.2 KEGG and GO enrichment analyses of DEGs

The clusterprofiler package was utilized to analyze the biological processes of DEGs. The cutoff of *P* value was set as < 0.05. In GO analysis, the up-regulated DEGs were mainly enriched in postsynapse assembly, postsynaptic density organization, extracellular structure organization, postsynaptic specialization organization, skeletal system development and regulation of canonical Wnt signaling pathway (Fig. 3A). The down-regulated DEGs were mostly enriched in response to glucocorticoid, toxic substance and corticosteroid, mononuclear cell migration, monocyte chemotaxis and negative regulation of cell migration (Fig. 3B). In the KEGG analysis, the up-regulated DEGs were highly enriched in ECM-receptor interaction, cell adhesion molecules (CAMs) and protein digestion and absorption (Fig. 3C), while the down-regulated ones were significantly enriched in complement and coagulation cascades, staphylococcus aureus infection, fluid shear stress and atherosclerosis, TNF signaling pathway, arachidonic acid metabolism and parathyroid hormone synthesis, secretion and action (Fig. 3D).

3.3 PPI network construction and clusters analyses

The PPI network was constructed via STRING, which included 267 nodes and 555 edges as shown in Fig. 4A. Then, we applied the plug-in MCODE of Cytoscape to find the most significant clusters in the network. With the criteria described above, 7 clusters were identified. The top 4 clusters were used for further analysis with k-core > 3. Cluster1 contains 24 nodes and 69 edges (Fig. 4B); Cluster2 contains 7 nodes and 13 edges (Fig. 4C); Cluster3 contains 4 nodes and 6 edges (Fig. 4D); Cluster4 contains 14 nodes and 24 edges (Fig. 4E). We performed GO analysis and KEGG analysis of these clusters by "clusterprofiler" respectively. Genes in cluster1 were mostly enriched in response to glucocorticoid (Fig. S3A) and Parathyroid hormone synthesis, secretion and action (Fig. S4A). The genes in cluster2 were mainly enriched in platelet degranulation (Fig. S3B) and adipocytokine signaling pathway (Fig. S4B). The genes in cluster3

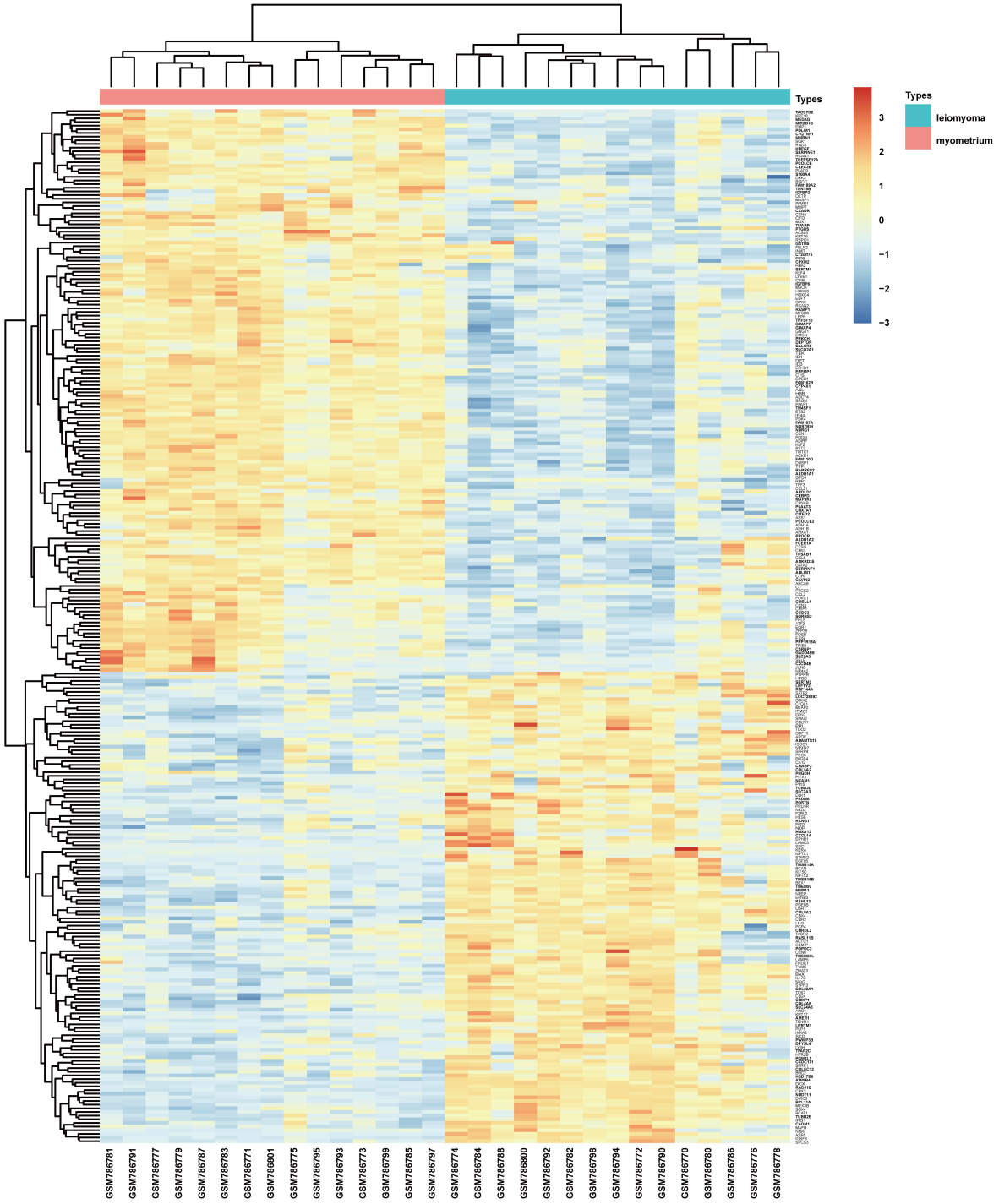

Fig. 2. Heatmap of the top 273 DEGs according to the value of |logFC| after deleting the samples GSM786796 and GSM786789.

were significantly enriched in postsynaptic density assembly (Fig. S3C) and nicotine addiction (Fig. S4C). The genes in cluster4 were largely enriched in extracellular matrix organization (Fig. S3D) and protein digestion and absorption (Fig. S4D).

3.4 Weighted co-expression network construction and module enrichment analyses

The "WGCNA" package was conducted in R language. Soft-thresholding power β = 30 (scale free R^2 = 0.96) was chosen to ensure a scale-free network (Fig. S5). A heatmap of module-traits relationships was constructed and 4 modules (blue, turquoise, purple, and tan modules) were extracted according to the *P* values (Fig. 5A,C) and the cut-off of *P*

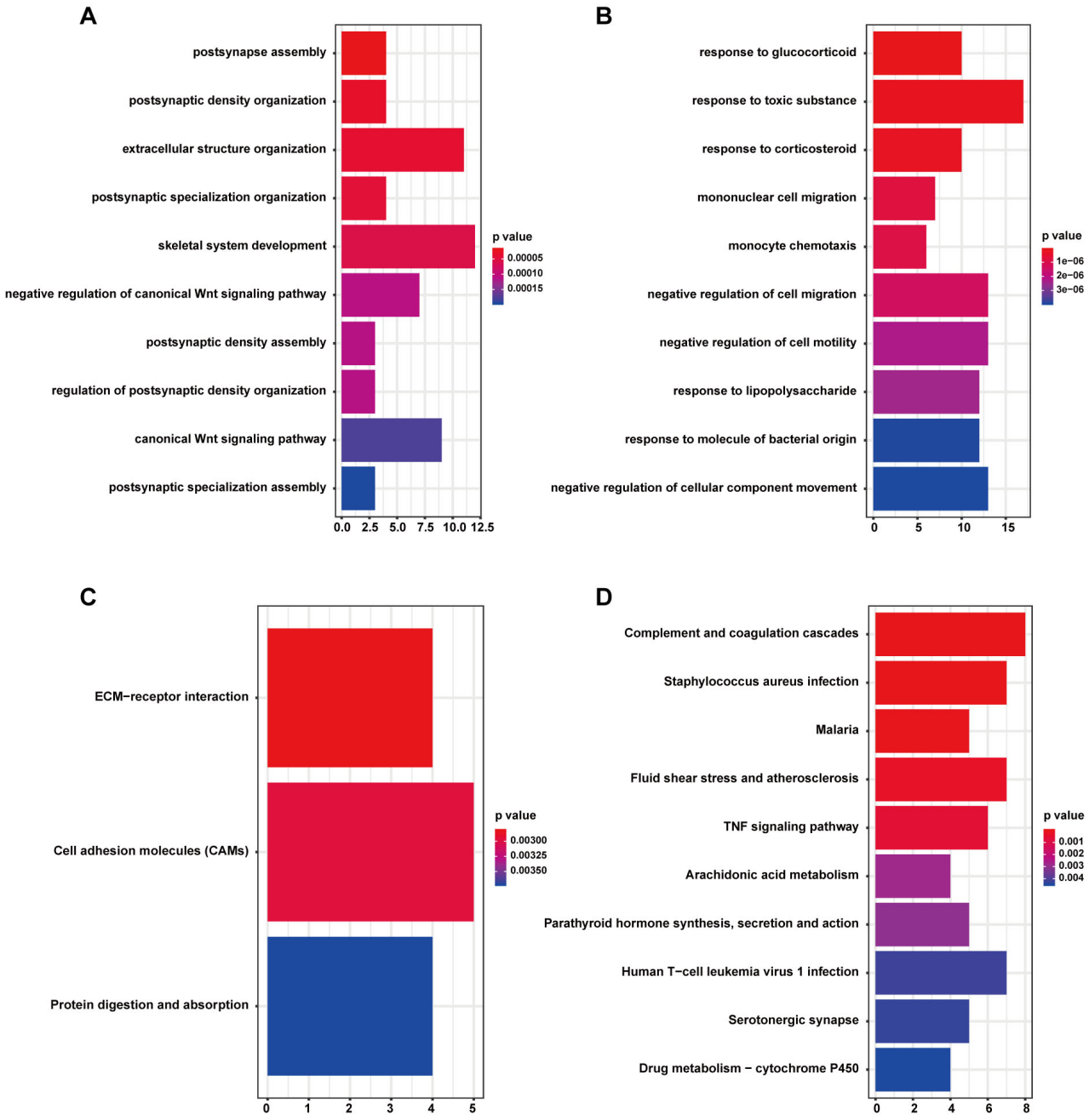

Fig. 3. KEGG and GO enrichment of DEGs. (A) GO enrichment of the up-regulated DEGs. (B) GO enrichment of the down-regulated DEGs. (C) KEGG analysis of the up-regulated DEGs. (D) KEGG analysis of the down-regulated DEGs.

value was < 0.01. Among these modules, blue module has the strongest correlation with uterine leiomyoma. Genes except those in grey module were identified for a heatmap (Fig. 5B).

To explore the connections and interactions among different modules, we completed a cluster analysis and calculated the connectivity of eigengenes. Results showed that 16 modules were divided into two major clusters. Intriguingly, blue, tan, purple, and cyan modules converged into one cluster (cluster1), while turquoise module was in another (cluster2) (Fig. 6A). In addition, there was a positive correlation among four modules in cluster1. However, these four modules were negatively correlated with turquoise module (Fig. 6B). Moreover, we analyzed GS (gene significance, which shows the correlation between the gene and the trait, uterine leiomyoma or normal myometrium) and MM (module membership, which reflects the correlation of the module eigengene and the gene expression profile) of the genes in the 5 modules respectively. The results demonstrated that 4 out of these 5 modules were statistically significant as shown in Fig. 7: blue module, cor = -0.79, $P = 9.1 \times 10\text{^}-67$ (Fig. 7A);

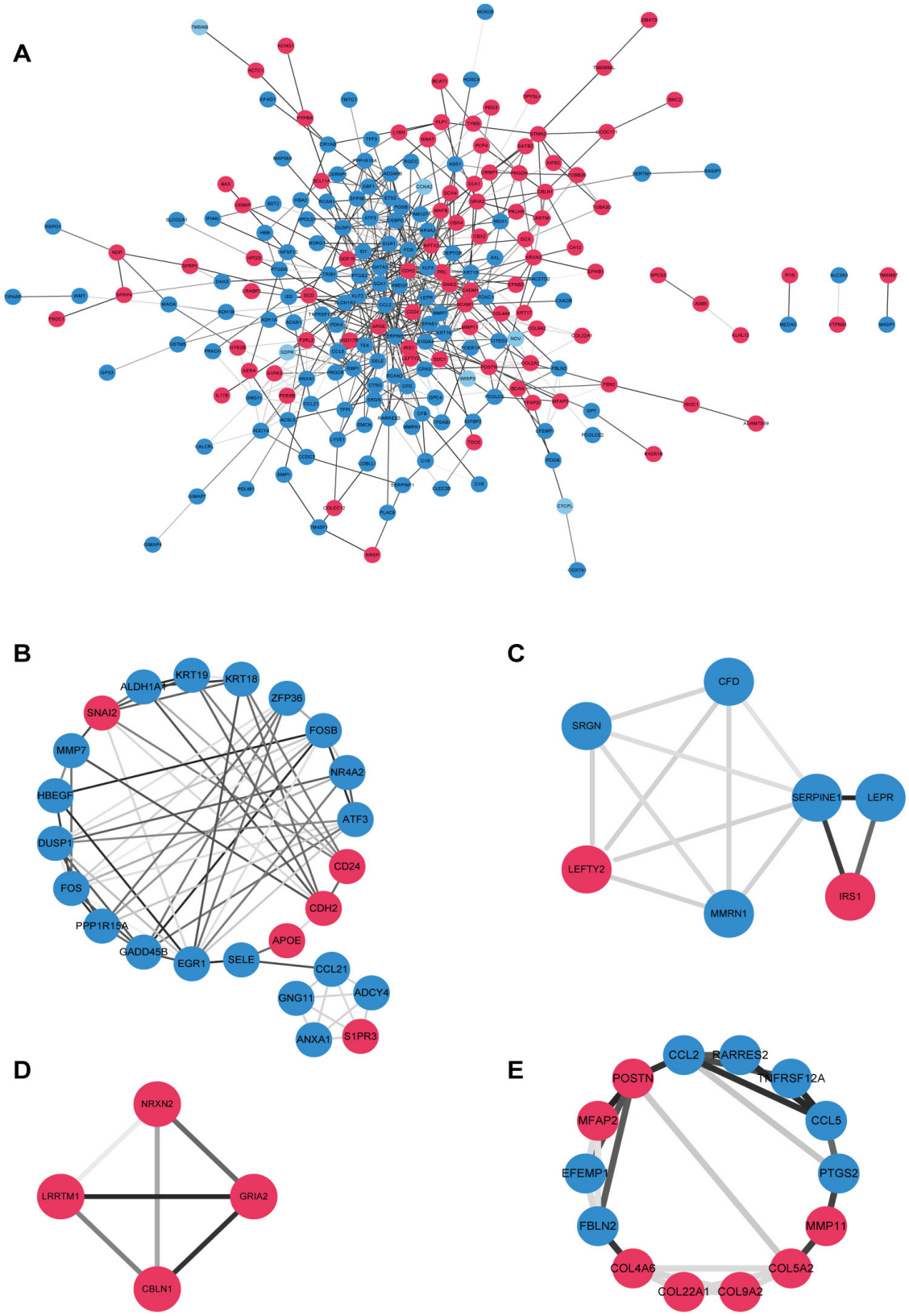

Fig. 4. PPI network construction and clusters analyses. The red nodes represent the up-regulated genes and the blue nodes represent the down-regulated genes. (A) The PPI network of 273 DEGs was constructed via STRING that contained 267 nodes and 555 edges. (B) Cluster rank 1. This cluster consists of 24 nodes and 69 edges and has the highest score in those clusters. (C) Cluster rank 2. (D) Cluster rank 3. (E) Cluster rank 4.

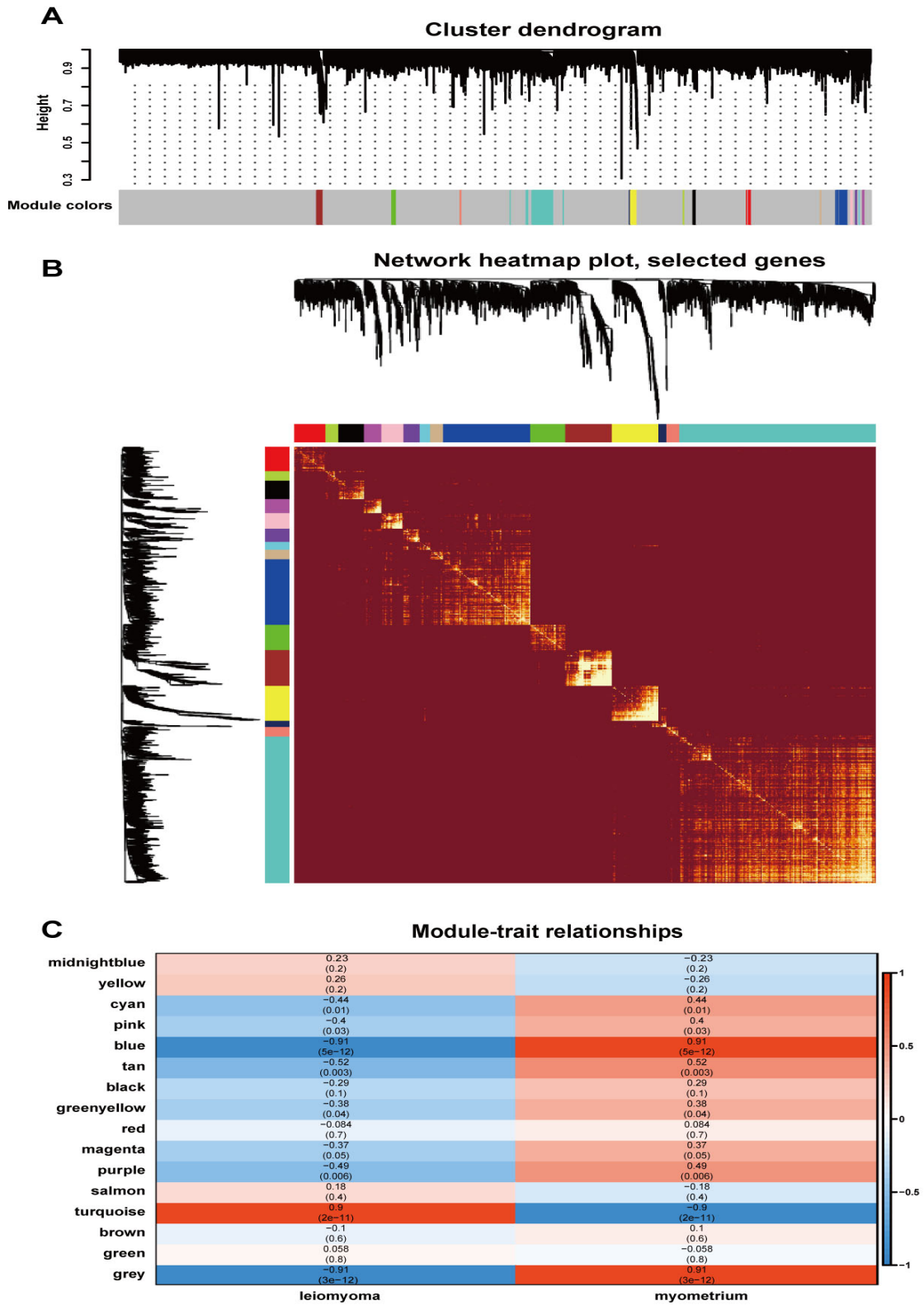

Fig. 5. Co-expression network creation and hub modules selection. (A) Dendrogram of all genes in GSE31699 clustered based on a dissimilarity measure (1-TOM). (B) A heatmap of selected genes. The intensity of the yellow color indicates the strength of the correlation between pairs of modules on a linear scale. (C) Correlation between modules and traits. The upper number in each cell refers to the correlation coefficient of each module in the trait, and the lower number is the corresponding *P*-value. Among them, the blue module was the most relevant modules with uterine leiomyoma traits.

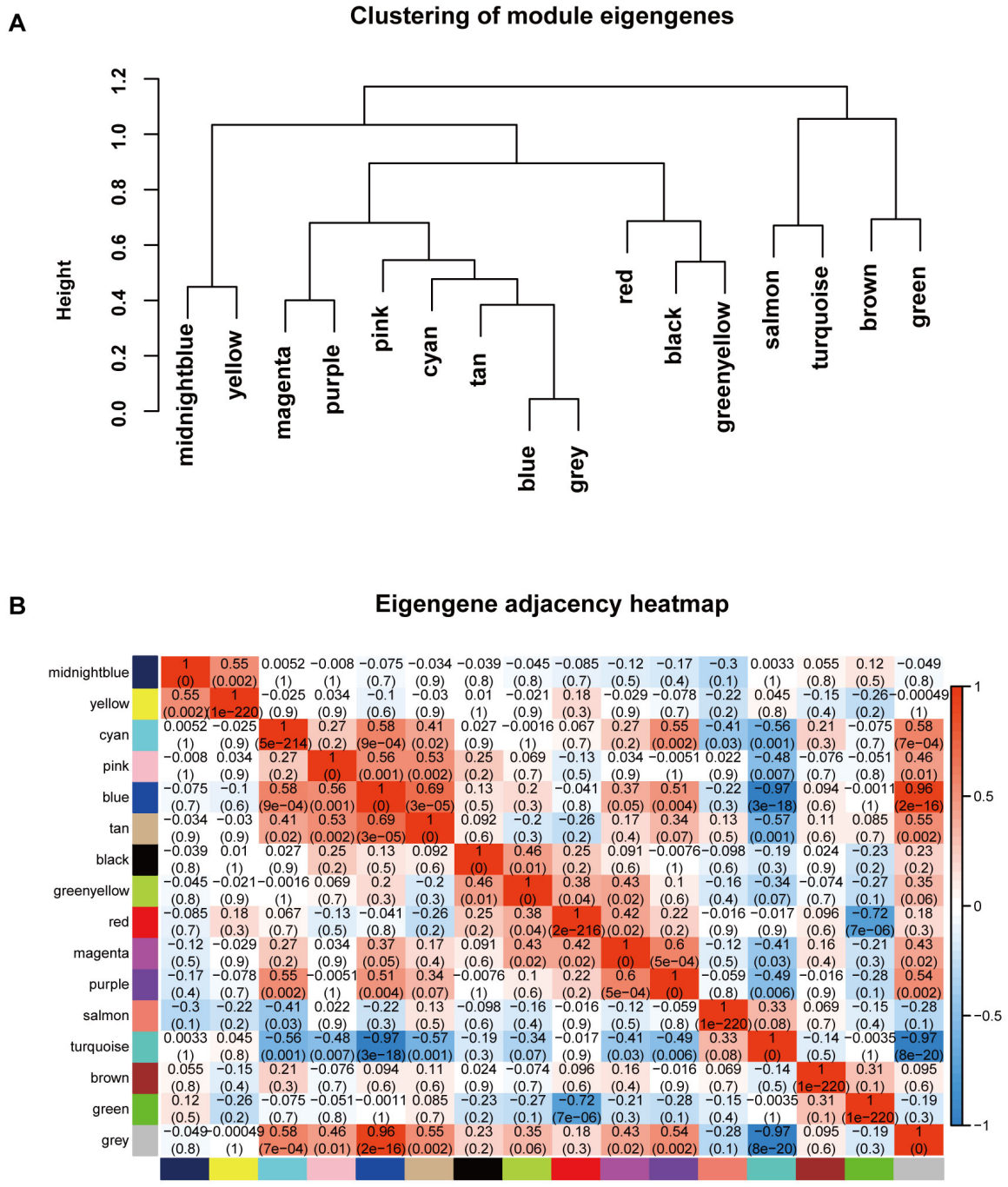

Fig. 6. Clustering of module eigengenes and eigengene adjacency heatmap (the red color indicates the strong correlation between different modules).

turquoise module, cor = 0.81, $P = 6.4 \times 10$^-161 (Fig. 7B); tan module, cor = -0.52, $P = 0.00025$ (Fig. 7C); cyan module, cor = -0.34, $P = 0.042$ (Fig. 7D). As the criteria was set as $P < 0.01$, we selected blue, turquoise and tan modules as hub modules.

Functional enrichment analyses of these modules were performed aiming to identify the underlying biological function and pathways those were related to uterine leiomyoma. After GO analysis, we discovered that genes in blue module were mainly enriched in DNA-dependent DNA replication, DNA replication initiation, planar cell polarity pathway involved in neural tube closure, G1/S transition of mitotic cell cycle and ATP-dependent chromatin remodeling (Fig. S6A). The genes in turquoise module were significantly enriched in regulation of vasculature development, regulation of inflammatory response, regulation of angiogenesis, regulation of cell-cell adhesion, cell-substrate adhesion, glomerulus development and response to peptide (Fig. S6C). The genes in tan

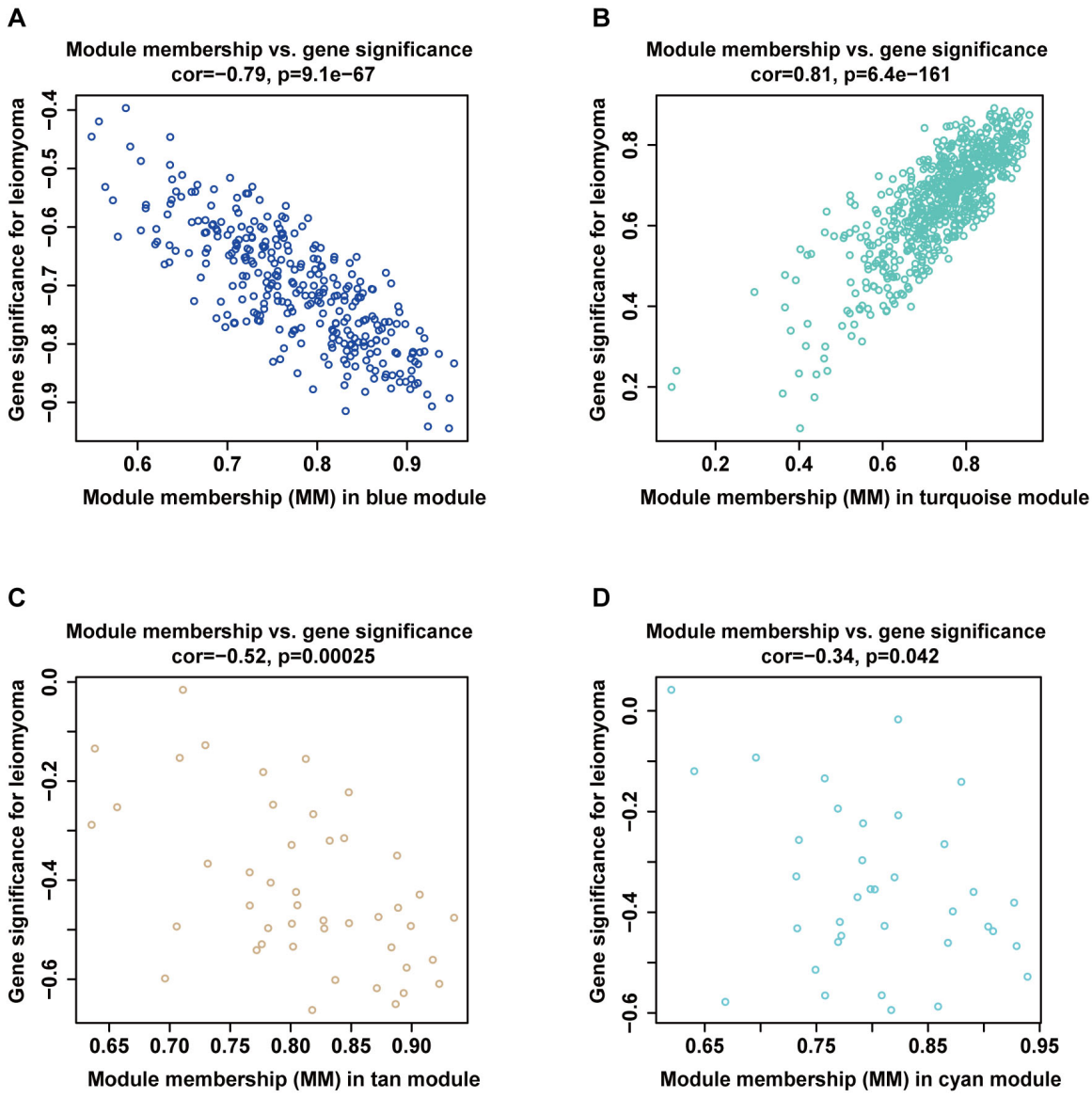

Fig. 7. Scatter plots of GS for uterine leiomyoma versus the MM in the hub modules. (A) Blue module. (B) Turquoise module. (C) Tan module. (D) Cyan module.

module were mostly enriched in extracellular matrix organization, cellular response to amino acid stimulus, protein heterotrimerization, extracellular structure organization, collagen fibril organization, response to amino acid, endodermal cell differentiation and collagen metabolic process (Fig. S6E).

Through the analysis of KEGG, we observed that genes in blue module were enriched in DNA replication, base excision repair, mismatch repair, cell cycle and nucleotide excision repair (Fig. S6B). Genes in turquoise module were enriched in *TNF* signaling pathway, Malaria, chemokine signaling pathway, fluid shear stress and atherosclerosis, viral protein interaction with cytokine and cytokine receptor, complement and coagulation cascades, *Rap1* signaling pathway and leukocyte trans-endothelial migration (Fig. S6D). The genes in tan module were enriched in ECM-receptor interaction, AGE-RAGE signaling pathway in diabetic complications, amoebiasis, focal adhesion, relaxin signaling pathway and *PI3K-Akt* signaling pathway (Fig. S6F).

3.5 PPI network construction of hub modules and identification of hub genes

We built a PPI network on the basis of STRING database for genes in the 3 hub modules by Cytoscape software independently. The blue module included 220 nodes and 647 edges (Fig. 8A). The turquoise module contained 592 nodes and 2710 edges (Fig. 8B). The tan module was compromised of 29 nodes and 78 edges (Fig. 8C).

In WGCNA, hub genes were highly connected in a module which may exert important biological functions. So, sorted by intramodular connectivity, the top 10% genes in each hub modules were selected as hub genes (30 out of 307

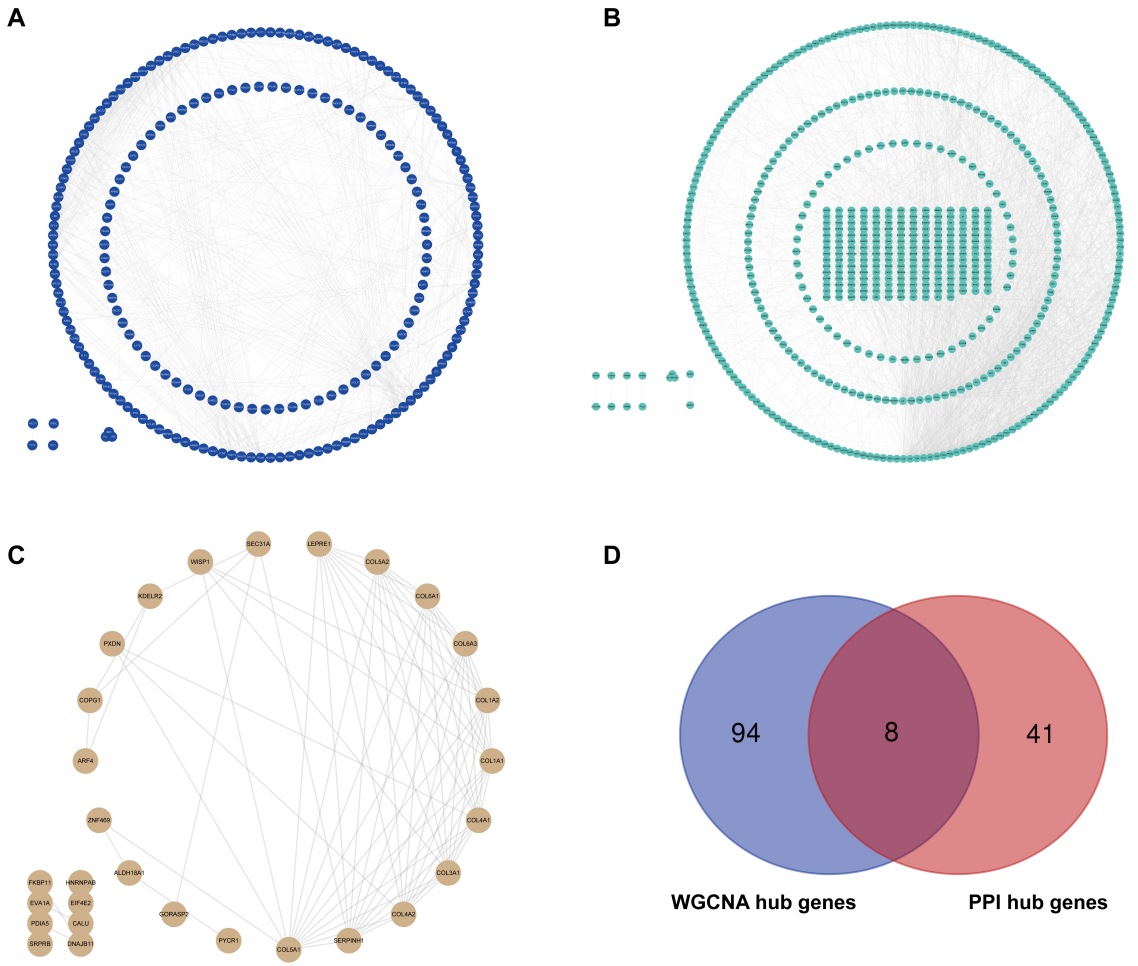

Fig. 8. PPI network construction of hub modules and identification of hub genes. (A) PPI network for genes in blue module. (B) PPI network for genes in turquoise module. (C) PPI network for genes in tan module. (D) Real hub genes belonging to both the hub modules and the hub clusters in PPI network of DEGs.

genes in blue module; 68 out of 687 genes in turquoise module; 4 out of 45 genes in tan module). According to the PPI network of DEGs constructed previously, we took 49 genes in 4 hub clusters as hub genes of DEGs' PPI network. Eventually, 8 hub genes were identified both in DEGs' PPI network and co-expression network. These 8 hub genes were regarded as "real" hub genes (Fig. 8D).

3.6 Hub genes validation

In the dataset GSE31699, 3 out of the 8 hub genes were up regulated while the other 5 genes were down-regulated in uterine leiomyoma compared to normal myometrium. We validated the expression of the selected hub genes in other datasets from GEO: GSE64763 [18], GSE764 [19] and GSE593 [20]. Eventually, we demonstrated that the expressions of *COL5A2*, *ALDH1A1*, *GNG11*, *EFEMP1* and *ANXA1* were also significantly different in these datasets in accordance with GSE31699 (Fig. 9). The mRNA expressions of these genes were analyzed by Oncomine database as shown in Fig. 10.

3.7 Gene set enrichment analysis

In order to confirm the potential enriched KEGG pathways of the 5 hub genes in uterine leiomyoma, we employed Gene set enrichment analysis of the five hub genes in GSE31699. Tow pathways of "base excision repair" and "complement and coagulation cascades" were mostly enriched ($P < 0.05$ and FDR < 0.25) (Fig. 11).

4. Discussion

In our study, we identified 273 DEGs related to uterine leiomyoma. GO analysis revealed that the upregulated DEGs were mainly enriched in extracellular structure organization, while the down-regulated DEGs were highly enriched in response to glucocorticoid and mononuclear cell migration. KEGG analysis suggested the upregulated genes were mostly enriched in ECM-receptor interaction. The down-regulated genes were mostly enriched in complement and coagulation cascades. The PPI network was constructed based on DEGs by STRING website and Cytoscape software. We identified 4 clusters when taking k-core $>$ 3 as a criterion.

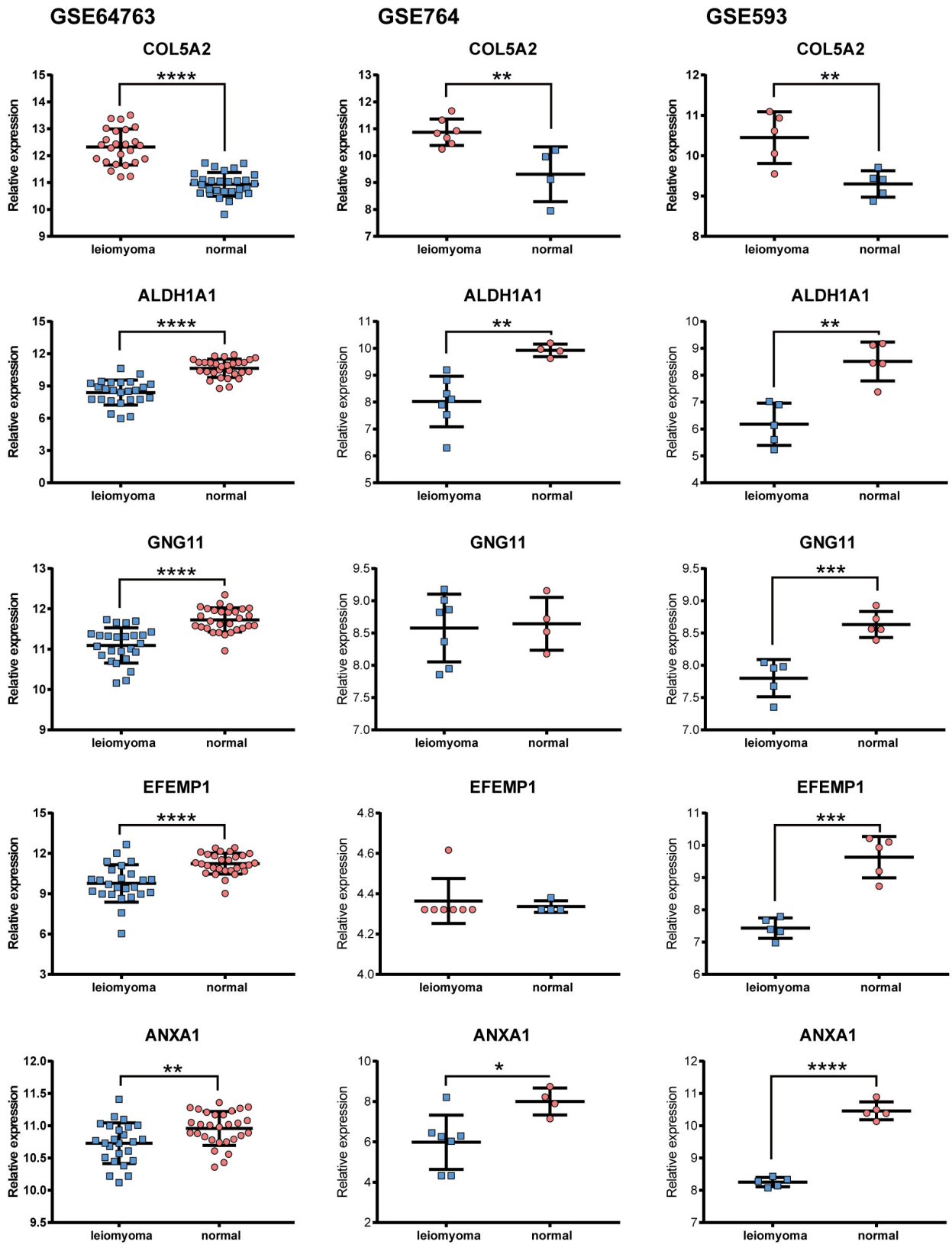

Fig. 9. The relative expression of hub genes in other datasets from GEO (GSE64763, GSE764 and GSE593, *: $P < 0.01$, **: $P < 0.001$, ***: $P < 0.0001$, ****: $P < 0.00001$).

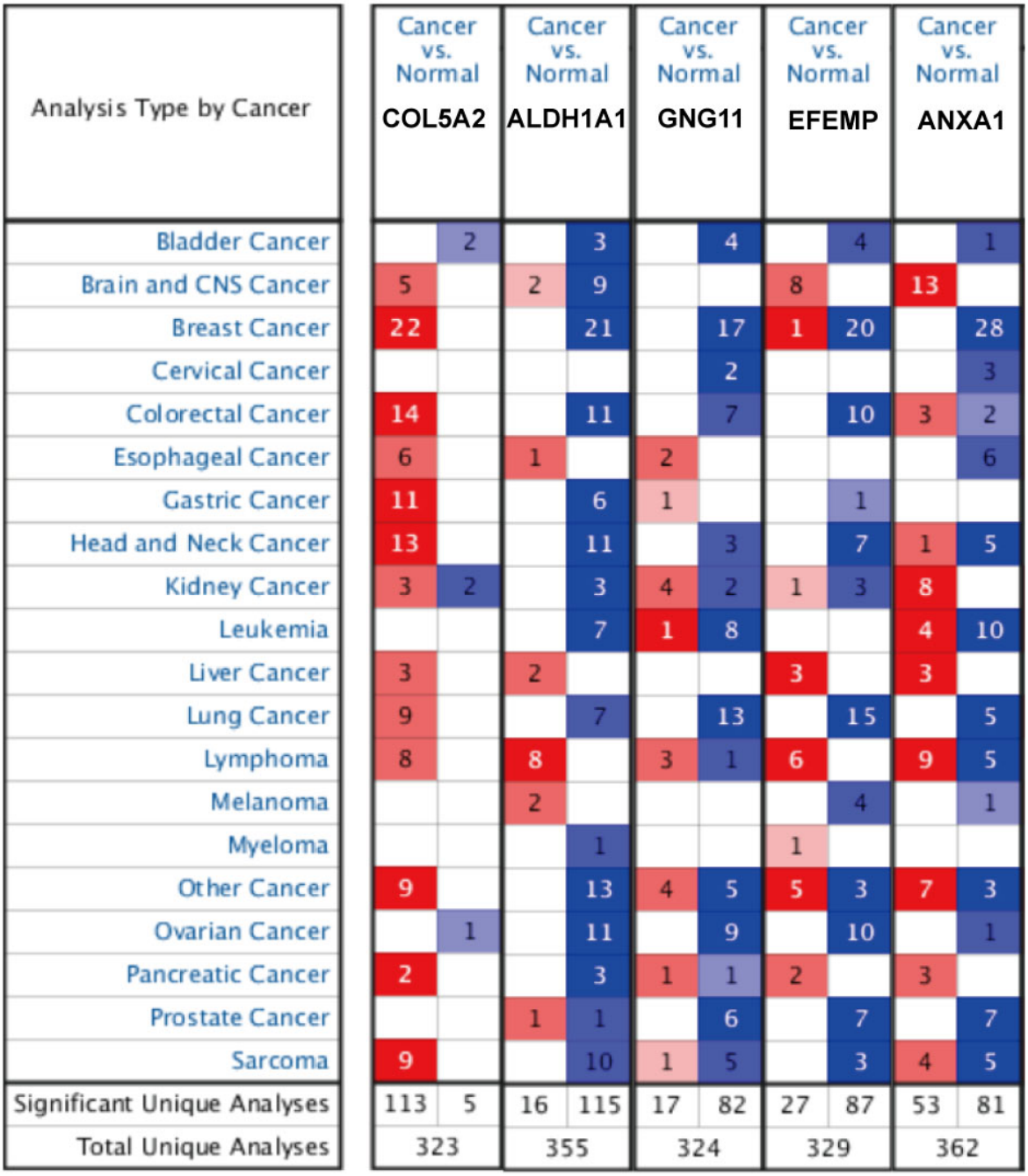

Analysis Type by Cancer	Cancer vs. Normal COL5A2		Cancer vs. Normal ALDH1A1		Cancer vs. Normal GNG11		Cancer vs. Normal EFEMP		Cancer vs. Normal ANXA1	
Bladder Cancer		2		3		4		4		1
Brain and CNS Cancer	5		2	9			8		13	
Breast Cancer	22			21		17	1	20		28
Cervical Cancer						2				3
Colorectal Cancer	14			11		7		10	3	2
Esophageal Cancer	6		1		2					6
Gastric Cancer	11			6	1			1		
Head and Neck Cancer	13			11		3		7	1	5
Kidney Cancer	3	2		3	4	2	1	3	8	
Leukemia				7	1	8			4	10
Liver Cancer	3		2				3		3	
Lung Cancer	9			7		13		15		5
Lymphoma	8		8		3	1	6		9	5
Melanoma			2					4		1
Myeloma				1			1			
Other Cancer	9			13	4	5	5	3	7	3
Ovarian Cancer		1		11		9		10		1
Pancreatic Cancer	2			3	1	1	2		3	
Prostate Cancer			1	1		6		7		7
Sarcoma	9			10	1	5		3	4	5
Significant Unique Analyses	113	5	16	115	17	82	27	87	53	81
Total Unique Analyses	323		355		324		329		362	

Fig. 10. Transcriptional expression of hub genes in 20 different types of cancer diseases (ONCOMINE database). 'Uterine corpus leiomyoma' was included in 'other cancer'. Difference of transcriptional expression was compared by students' *t*-test. Cut-off of *P* value and fold change were as following: *P* value: 0.01, fold change: 1.5, gene rank: 10%, data type: mRNA. The number in cell means how many studies in the database meet the threshold. Red means higher expression in cancer while blue means lower expression.

In WGCNA analysis, we selected 4 hub modules. The turquoise module had the highest correlation which contains 687 genes. GO analysis showed that the genes were mostly enriched in regulation of vasculature development. In KEGG analysis, they were significantly enriched in TNF signaling pathway. We selected 102 genes, which were the top 10% genes according to the intramodular connectivity in each hub module. In view of the PPI network, 8 genes were screened as the hub genes. 5 out of these genes (*COL5A2, ALDH1A1, GNG11, EFEMP1* and *ANXA1*) were validated by other GEO datasets and Oncomine database. The results indicated that the 5 hub genes may be implicated in the pathology of uterine leiomyoma.

17 whose mutations in this gene are associated with Ehlers-Danlos syndrome. In this study, we found that the expression of *COL5A2* in uterine leiomyoma was high in com-

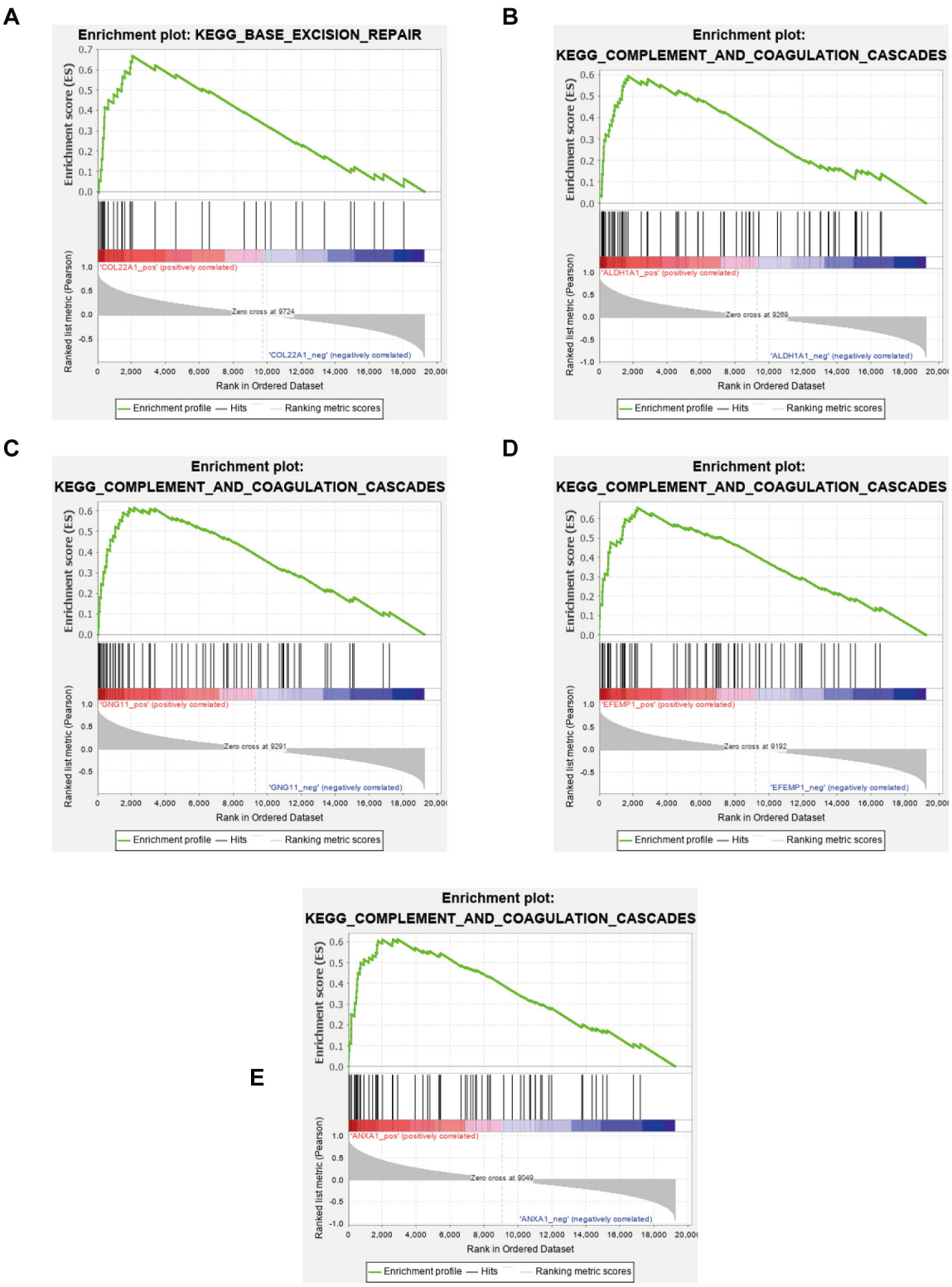

Fig. 11. Gene set enrichment analysis (GSEA) using GSE31699. The most enriched functional gene set in uterine leiomyoma samples with hub genes highly expressed was identified. (A) COL5A2. (B) ALDH1A1. (C) GNG11. (D) EFEMP1. (E) ANXA1.

parison to normal myometrium. Accumulation of extracellular matrix is a specific cause of uterine leiomyoma, and collagen is a key structure component of ECM. Many subtypes of collagen were proved to have higher levels such as *COL1A1*, *4A2*, *6A1*, *6A2*, *7A1* and *16A1* [21], while *COL5A2* has not been validated. The up-regulated DEGs of GSE31699

and tan module including *COL5A2* in WGCNA analysis were significantly enriched in extracellular structure organization. Besides, in our GSEA analysis, the functions of *COL5A2* were mostly enriched in extra matrix structure constituent and collagen fibril organization. So, we hypothesize that *COL5A2* may also be implicated in the pathological process of uterine leiomyoma. In addition, Giri and colleagues found that the region in chromosome 2q31-32 including *COL5A2* may mediate interaction between local ancestry and BMI, which were risk factors for uterine leiomyoma [22]. Oncomine database demonstrated overexpression of *COL5A2* in several cancers which indicated its potential role in other cancers. Furthermore, some studies showed that *COL5A2* was correlated with poor clinical outcomes of bladder and gastric cancer patients while the detailed mechanisms still await clarification [23, 24].

The protein encoded by *ALDH1A1* belongs to the aldehyde dehydrogenase family, which is commonly known as a major participant in alcohol metabolism. There have been controversies about the effect of *ALDH1A1* on uterine leiomyoma. Zaitseva and coworkers found that αSMA-negative fibroblast-like cells of the connective tissue strongly expressed *ALDH1A1* in myometrium when compared with uterine leiomyoma [25], which was consist with the research of Xia and colleagues [26]. *ALDH1A1* expression was regulated differently in myometrial and fibroid cells by retinol metabolism pathway which may be important in fibroid pathophysiology [27]. In another study, Shveiky and co-investigators demonstrated an increased level of the *ALDH1A1* protein in uterine leiomyoma, while acetaldehyde could inhibit the growth of uterine leiomyoma cells [28]. In our study, the genes positively correlated with *ALDH1A1* in GSEA31699 were enriched in fibrinolysis, a process that solubilizes fibrin in the bloodstream. And in WGCNA analysis, the genes in turquoise module containing *ALDH1A1* were significantly enriched in regulation of vasculature development. So, we make an assumption that *ALDH1A1* may play a role in improving the blood perfusion of uterine leiomyoma. More detailed mechanisms should be explored to validate our hypothesis.

GNG11 is a member of the guanine nucleotide-binding protein (G protein) gamma family and encodes a lipid-anchored, cell membrane protein, which plays a role in transmembrane signaling system [29]. Our results demonstrated *GNG11* was down-regulated in uterine leiomyoma. Oncomine database showed that *GNG11* had lower level in malignant tumors, especially breast cancer and lung cancer, when compared with normal tissues. Studies have pinpointed that *GNG11* may be a biomarker for lung adenocarcinoma and acute myeloid leukemia subtype classification, and lower expression of *GNG11* in lung cancer indicated poor prognosis [30, 31]. Yet the knowledge of mechanisms how *GNG11* exerts biological functions is still limited. Previous studies showed that *GNG11* could suppress cell growth by inducing reactive oxygen species and regulate cellular senescence by activating *ERK1/2* of the *MAP* kinase family [32, 33]. GSEA analysis in this study also showed that the genes positively correlated with *GNG11* mostly enriched in regulation of necrotic cell death, which indicated that lower expression of *GNG11* in uterine leiomyoma may contribute to cell proliferation.

EFEMP1 (EGF containing fibulin extracellular matrix protein 1) contains tandemly repeated epidermal growth factor-like repeats followed by a C-terminus fibulin-type domain. *EFEMP1* encoded the protein Fibulin-3, which may act as an antagonist of angiogenesis or may promote tumor growth. We found that *EFEMP1* was down-regulated in uterine leiomyoma based on the datasets. Marsh *et al.* confirmed the significant down-regulation in leiomyoma both *in vivo* and *in vitro*, which was consistent with other studies on *EFEMP1* expression in other solid tumors [34]. In this study, we utilized Oncomine database and discovered that *EFEMP1* was down regulated in several kinds of solid cancers. Hu *et al.* demonstrated that *EFEMP1* had the capacity to suppressed the growth of hepatocellular carcinoma (HCC) cells, while its decreased expression was related to the extent of spread to the lymph nodes and the prognosis of patients with HCC [35]. Further study suggested that lower level of *EFEMP1* expression maybe caused by the hypermethylation in the promoter region, while additional researches are warranted to explore the role of *EFEMP1* in uterine leiomyoma pathology.

ANXA1 encodes a membrane-localized protein. This protein binds phospholipids and inhibits phospholipase A2 to serve a role in anti-inflammatory. According to Oncomine database, loss of function or expression of this gene has been detected in multiple tumors including uterine leiomyoma, while overexpression was also found in many cancers of the gut [36, 37]. *ANXA1* may play protective antitumorigenic roles or promote metastasis and invasion depending on the type of cancer and cancer grade [38]. Anjum and coworkers used Next-generation RNA Sequencing to discover that *ANXA1* has lower level in uterine leiomyoma than in normal tissues, being confirmed by Real-Time PCR further [39]. *ANXA1* is involved in several cellular signal transduction pathways, especially those related to inflammation, cell differentiation, proliferation and migration [40]. In the present study, the GSEA analysis revealed that the genes positively correlated with *ANXA1* significantly enriched in vasculogenesis and blood vessel endothelial cell migration, indicating that *ANXA1* may be involved in the angiogenesis during the development of uterine leiomyoma. However, more detailed mechanisms of *ANXA1* for the growth of uterine fibroids still await elucidation.

There were some limitations in our study. Firstly, all the data analyzed in our study was obtained from the online databases, further studies including larger quantity of clinical specimens are required to validate our findings. Secondly, as uterine leiomyomas are commonly benign tumors, there were not enough clinical data in GEO or TCGA database, so survival analysis could not be conducted in this study. The

clinical importance of these genes should be assessed in the future. Finally, we did not clarify the roles of the hub genes in uterine leiomyomas. Future basic researches are worth being undertaken to elucidate the underlying mechanisms.

In conclusion, by using the analysis of bioinformatics, we found that *COL5A2*, *ALDH1A1*, *GNG11*, *EFEMP1* and *ANXA1* might be the pivotal genes for the pathogenesis of uterine leiomyomas by participating in the pathways of ECM accumulation, vasculature development, angiogenesis and cell proliferation. These genes may be related to the progression of uterine leiomyomas or be the therapeutic targets. The present findings probably provide us with a new perspective on diagnosis and therapy of uterine leiomyomas. However, the screened genes and pathways still need to be confirmed.

Author contributions

Jie Wu and Yu-Jie Sun conceived and designed the study; Yi-Chao Jin, Tong-Hui Ji, Xiong Yuan and Ying Sun performed the data analysis, Yi-Chao Jin and Tong-Hui Ji wrote the paper.

Acknowledgment

We would like to express our gratitude to all those who gave us suggestions and instructions during the writing of this manuscript. And thanks all the peer reviewers and editors for their opinions and suggestions.

Conflict of interest

The authors declare no competing interests.

Supplementary material

Supplementary material associated with this article can be found, in the online version, at https://ejgo.imrpress.com/EN/10.31083/j.ejgo.2021.01.2151.

References

[1] Bulun SE. Uterine fibroids. New England Journal of Medicine. 2013; 369: 1344-1355.

[2] Giuliani E, As-Sanie S, Marsh EE. Epidemiology and management of uterine fibroids. International Journal of Gynecology & Obstetrics. 2020; 149: 3-9.

[3] Baranov VS, Osinovskaya NS, Yarmolinskaya MI. Pathogenomics of uterine fibroids development. International Journal of Molecular Sciences. 2019; 20: 6151.

[4] Stewart EA, Laughlin-Tommaso SK, Catherino WH, Lalitkumar S, Gupta D, Vollenhoven B. Uterine fibroids. Nature Reviews Disease Primers. 2016; 2: 16043.

[5] Islam MS, Ciavattini A, Petraglia F, Castellucci M, Ciarmela P. Extracellular matrix in uterine leiomyoma pathogenesis: a potential target for future therapeutics. Human Reproduction Update. 2018; 24: 59-85.

[6] McWilliams MM, Chennathukuzhi VM. Recent advances in uterine fibroid etiology. Seminars in Reproductive Medicine. 2017; 35: 181-189.

[7] Liu X, Liu Y, Zhao J, Liu Y. Screening of potential biomarkers in uterine leiomyomas disease via gene expression profiling analysis. Molecular Medicine Reports. 2018; 17: 6985-6996.

[8] Kim YJ, Kim YY, Shin JH, Kim H, Ku SY, Suh CS. Variation in MicroRNA Expression Profile of Uterine Leiomyoma with Endometrial Cavity Distortion and Endometrial Cavity Non-Distortion. International Journal of Molecular Sciences. 2018; 19: 2524.

[9] Langfelder P, Horvath S. WGCNA: an R package for weighted correlation network analysis. BMC Bioinformatics. 2009; 9: 559.

[10] Ritchie ME, Phipson B, Wu D, Hu Y, Law CW, Shi W, *et al.* Limma powers differential expression analyses for RNA-sequencing and microarray studies. Nucleic Acids Research. 2015; 43: e47-e47.

[11] Yu G, Wang L, Han Y, He Q. ClusterProfiler: an R package for comparing biological themes among gene clusters. A Journal of Integrative Biology. 2012; 16: 284-287.

[12] Szklarczyk D, Franceschini A, Wyder S, Forslund K, Heller D, Huerta-Cepas J, *et al.* STRING v10: protein-protein interaction networks, integrated over the tree of life. Nucleic Acids Research. 2015; 43: D447-D452.

[13] Shannon P. Cytoscape: a software environment for integrated models of biomolecular interaction networks. Genome Research. 2003; 13: 2498-2504.

[14] Bader GD, Hogue CWV. An automated method for finding molecular complexes in large protein interaction networks. BMC Bioinformatics. 2003; 4: 2.

[15] Horvath S, Dong J. Geometric interpretation of gene coexpression network analysis. PLoS Computational Biology. 2008; 4: e1000117.

[16] Subramanian A, Tamayo P, Mootha VK, Mukherjee S, Ebert BL, Gillette MA, *et al.* Gene set enrichment analysis: a knowledge-based approach for interpreting genome-wide expression profiles. Proceedings of the National Academy of Sciences. 2005; 102: 15545-15550.

[17] Mootha VK, Lindgren CM, Eriksson K-F, Subramanian A, Sihag S, Lehar J, *et al.* PGC-1α-responsive genes involved in oxidative phosphorylation are coordinately downregulated in human diabetes. Nature Genetics. 2003; 34: 267-273.

[18] Barlin JN, Zhou QC, Leitao MM, Bisogna M, Olvera N, Shih KK, *et al.* Molecular subtypes of uterine leiomyosarcoma and correlation with clinical outcome. Neoplasia. 2015; 17: 183-189.

[19] Quade BJ, Wang T, Sornberger K, Dal Cin P, Mutter GL, Morton CC. Molecular pathogenesis of uterine smooth muscle tumors from transcriptional profiling. Genes, Chromosomes & Cancer. 2004; 40: 97-108.

[20] Hoffman PJ, Milliken DB, Gregg LC, Davis RR, Gregg JP. Molecular characterization of uterine fibroids and its implication for underlying mechanisms of pathogenesis. Fertility and Sterility. 2004; 82: 639-649.

[21] Malik M, Norian J, McCarthy-Keith D, Britten J, Catherino W. Why leiomyomas are called fibroids: the central role of extracellular matrix in symptomatic women. Seminars in Reproductive Medicine. 2010; 28: 169-179.

[22] Giri A, Edwards TL, Hartmann KE, Torstenson ES, Wellons M, Schreiner PJ, *et al.* African genetic ancestry interacts with body mass index to modify risk for uterine fibroids. PLoS Genetics. 2017; 13: e1006871.

[23] Zeng X, Liu X, Liu T, Wang X. The clinical significance of COL5a2 in patients with bladder cancer: a retrospective analysis of bladder cancer gene expression data. Medicine. 2018; 97: e0091.

[24] Cao L, Chen Y, Zhang M, Xu D, Liu Y, Liu T, *et al.* Identification of hub genes and potential molecular mechanisms in gastric cancer by integrated bioinformatics analysis. PeerJ. 2019; 6: e5180.

[25] Zaitseva M, Vollenhoven BJ, Rogers PAW. Retinoic acid pathway genes show significantly altered expression in uterine fibroids when compared with normal myometrium. Molecular Human Reproduction. 2007; 13: 577-585.

[26] Xia L, Liu Y, Fu Y, Dongye S, Wang D. Integrated analysis reveals candidate mRNA and their potential roles in uterine leiomyomas. Journal of Obstetrics and Gynaecology Research. 2017; 43: 149-156.

[27] Zaitseva M, Vollenhoven BJ, Rogers PAW. Retinoids regulate genes involved in retinoic acid synthesis and transport in human myometrial and fibroid smooth muscle cells. Human Reproduction. 2008; 23: 1076-1086.

[28] Shveiky D, Shushan A, Ben Bassat H, Klein BY, Ben Meir A, Levitzky R, *et al*. Acetaldehyde differentially affects the growth of uterine leiomyomata and myometrial cells in tissue cultures. Fertility and Sterility. 2009; 91: 575-579.
[29] Downes GB, Gautam N. The G protein subunit gene families. Genomics. 1999; 62: 544-552.
[30] Yang G, Chen Q, Xiao J, Zhang H, Wang Z, Lin X. Identification of genes and analysis of prognostic values in nonsmoking females with non-small cell lung carcinoma by bioinformatics analyses. Cancer Management and Research. 2019; 10: 4287-4295.
[31] Haouas H, Haouas S, Uzan G, Hafsia A. Identification of new markers discriminating between myeloid and lymphoid acute leukemia. Hematology. 2010; 15: 193-203.
[32] Takauji Y, Kudo I, En A, Matsuo R, Hossain MN, Nakabayashi K, *et al*. GNG11 (G-protein subunit γ 11) suppresses cell growth with induction of reactive oxygen species and abnormal nuclear morphology in human SUSM-1 cells. Biochemistry and Cell Biology. 2017; 95: 517-523.
[33] Hossain MN, Sakemura R, Fujii M, Ayusawa D. G-protein gamma subunit GNG11 strongly regulates cellular senescence. Biochemical and Biophysical Research Communications. 2006; 351: 645-650.
[34] Marsh EE, Chibber S, Wu J, Siegersma K, Kim J, Bulun S. Epidermal growth factor-containing fibulin-like extracellular matrix protein 1 expression and regulation in uterine leiomyoma. Fertility and Sterility. 2016; 105: 1070-1075.
[35] Hu J, Duan B, Jiang W, Fu S, Gao H, Lu L. Epidermal growth factor-containing fibulin-like extracellular matrix protein 1 (EFEMP1) suppressed the growth of hepatocellular carcinoma cells by promoting Semaphorin 3B(SEMA3B). Cancer Medicine. 2019; 8: 3152-3166.
[36] Sheu M, Li C, Lin C, Lee S, Lin L, Chen T, *et al*. Overexpression of ANXA1 confers independent negative prognostic impact in rectal cancers receiving concurrent chemoradiotherapy. Tumor Biology. 2014; 35: 7755-7763.
[37] Duncan R, Carpenter B, Main LC, Telfer C, Murray GI. Characterisation and protein expression profiling of annexins in colorectal cancer. British Journal of Cancer. 2008; 98: 426-433.
[38] Foo SL, Yap G, Cui J, Lim LHK. Annexin-A1 - a blessing or a curse in cancer? Trends in Molecular Medicine. 2019; 25: 315-327.
[39] Anjum S, Sahar T, Nigam A, Wajid S. Transcriptome analysis of mRNA in uterine leiomyoma using next-generation RNA sequencing. Anti-Cancer Agents in Medicinal Chemistry. 2019; 19: 1703-1718.
[40] Guo C, Liu S, Sun M. Potential role of Anxa1 in cancer. Future Oncology. 2013; 9: 1773-1793.